THE JOURNAL OF PHYSICAL CHEMISTRY C
A JOURNAL OF THE AMERICAN CHEMICAL SOCIETY

pubs.acs.org/JPCC

Article

Ultrafast Spectral Signatures of Laser-Induced Chalcogen Vacancies in MoS_2

Clare L. Keenan, Ashley Arcidiacono, Nasim Mirzajani, Cooper R. Johnston, and Sarah B. King*

Cite This: *J. Phys. Chem. C* 2024, 128, 17536−17542

Read Online

ACCESS | Metrics & More | Article Recommendations | Supporting Information

ABSTRACT: Monolayer transition metal dichalcogenides have a variety of unique properties—mechanical flexibility, bandgaps in the visible region, strain tunability, and more—making them viable candidates for a range of applications, including optoelectronic and spintronic devices. Optical probes such as lasers are frequently used to characterize the electronic structure and dynamics of these systems to facilitate device engineering. Critical to the interpretation of such experiments is the ability to distinguish intrinsic sample responses from measurement-induced sample modification or damage. Here, we report laser-induced trion formation in MoS_2 monolayers via the in situ formation of sulfur vacancies. Real-time laser exposure experiments reveal that spectra are significantly modified on the order of seconds of laser irradiation. Ultrafast time-resolved experiments on irradiated samples show that the intrinsic neutral excitons can appear with an apparent time delay with respect to laser-induced trions. This delayed behavior is particularly susceptible to being improperly assigned as, for example, charge transfer in a heterostructure system, and must therefore be considered in future studies of TMDs, TMD heterostructures, and similar systems.

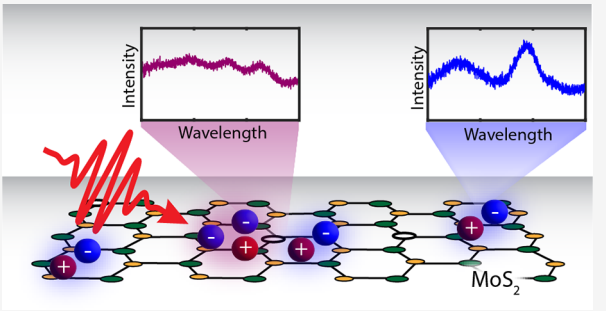

INTRODUCTION

Monolayer van der Waals materials and their heterostructures are popular systems for modern electronics and device design. Their mechanical flexibility, modularity, and electronic tunability makes them well suited to a variety of applications such as catalysis, sensing, and micro- and nanoelectronics.[1−9] Monolayer transition metal dichalcogenides (TMDs) are a particularly popular subset of these systems given their direct band gaps with energies in the visible region, and spin-valley polarization.[2,10−12] Understanding the electronic structure and dynamics of these systems is critical to driving informed engineering and optimization, as well as investigating fundamental scientific questions. In TMD systems, electronic transitions in the visible region are dominated by A and B excitons at the K/K′ valleys. Efforts toward the characterization of the electronic structure of TMDs and TMD heterostructure systems are typically focused on the properties of these excitons and related quasi-particles such as trions (charged excitons) and biexcitons.[13−24]

Accurate and predictive understanding of a material's electronic structure requires that any experimental probe not alter the system during measurement; however, this is sometimes challenging. Probes of electronic structure often involve irradiation with pulsed photon sources. Time-resolved stroboscopic experiments, in particular, can require laser irradiation of a sample over an extended period of time. These conditions are potentially damaging, and experiments often require careful tuning to find the ideal intensity conditions to produce high quality data without risking modification or damage of the sample under study. Therefore, it is important that we identify the characteristics of sample damage, particularly when these characteristics are subtle and could be misidentified as novel physics.

In this paper, we report the spectral signatures of laser-induced sulfur vacancies in monolayer MoS_2 in real-time laser exposure and transient absorption experiments. We demonstrate that even gentle irradiation can result in a modification of time-resolved difference spectra. In the visible region, monolayer MoS_2 intrinsically has two well resolved electronic transitions representing the formation of A and B excitons. In contrast, following laser irradiation, we observe two pairs of bleached features. In transient absorption measurements, we observe that one pair that appears instantaneously with the pump, and one that appears with a pump−probe time delay. This behavior is not intrinsic to the sample, but rather induced by laser exposure. Our work suggests that laser irradiation generates sulfur vacancy defects, which support the formation of negative trions. These negative trions appear in the

Received: June 26, 2024
Revised: August 30, 2024
Accepted: September 25, 2024
Published: October 4, 2024

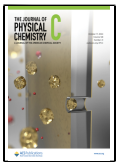

https://doi.org/10.1021/acs.jpcc.4c04253
J. Phys. Chem. C 2024, 128, 17536−17542

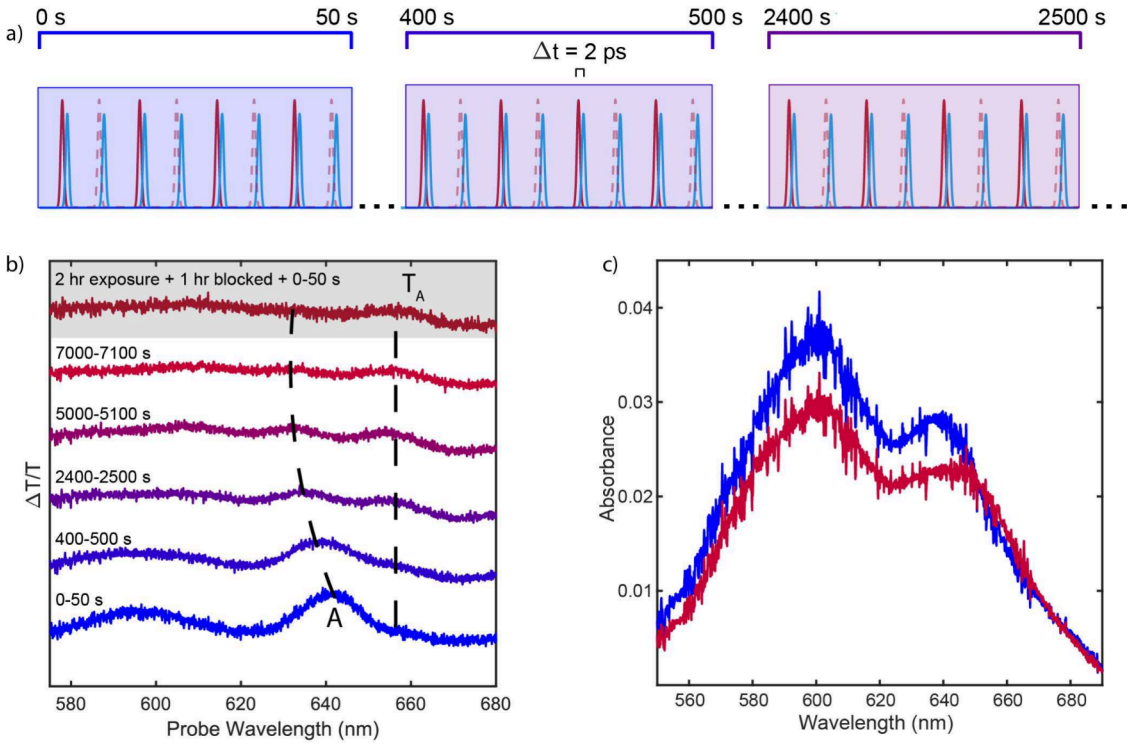

Figure 1. Effect of laser exposure on monolayer MoS_2. (a) Experimental schematic depicting three of the six regimes depicted in (b). Blue pulses represent the probe, red solid pulses represent the pump, red dashed pulses represent a blocked pump. (b) Difference spectra collected at 2 ps pump−probe time delay at increasing pump exposure times. Data are averaged over the pump exposure times indicated above each spectrum. Spectra are offset for clarity. (c) Static absorption spectra collected before (blue) and after (red) the laser exposure experiment.

presented spectra as additional peaks. While the severity of this behavior is certainly affected by sample quality and experimental conditions, and is commonly not present to a measurable degree,[17,22,25−28] characterizing this laser-induced behavior is important so that it may be considered as a possibility when making time-resolved spectroscopic assignments. Relevant sample traits such as defect density and grain size are difficult to control in the preparation of TMDs via both chemical vapor deposition and exfoliation.[2] It may therefore be impossible to control or determine *a priori* whether this laser-induced behavior is expected at a detectable level for a given sample. Understanding of these signatures is required in order to accurately distinguish between induced and intrinsic behavior.

METHODS

Laser Exposure Experiments. Real-time laser exposure experiments were conducted using two optical parametric amplifiers (OPAs) (Light Conversion Orpheus-N-3H and Orpheus-N-2H) pumped by a Yb:KGW laser centered at 1030 nm (Light Conversion Pharos PH2) running at a repetition rate of 50 kHz. OPA outputs have pulse durations of 20−40 fs. A supercontinuum probe (~500−800 nm, 1.55−2.48 eV) was generated by focusing one OPA output centered at 800 nm into a 5 mm thick YAG crystal. The other OPA output served as the pump and was centered on 575 nm and set at a fluence of 10 $\mu J/cm^2$. This fluence was chosen to be representative of typical fluences used in pulsed optical experiments on similar systems. The pump is directed through an optical chopper (Thorlabs MC2000B) that is synchronized to the laser pulse train and running at 6.25 kHz. Pump and probe were focused onto a sample of monolayer MoS_2 on a fused silica substrate (see Sample Preparation section) held at 78 K in an optical cryostat with the sample space held under low vacuum (~10^{-3} Torr) (Andor Oxford Instruments OptiStat DNV). The pump−probe time delay was set at 2 ps using a motorized linear stage (Newport GTS-150). After transmitting through the sample, the probe was recollimated and then dispersed by a diffraction grating (Thorlabs) onto a CMOS line scan camera (JAI SW-4000-PMCL). The dispersed probe was strategically positioned on the camera in order to exclude intense regions near the seed wavelength which contain no useful spectral information. Camera pixel number was calibrated to wavelength using a series of bandpass filters (Thorlabs). A small portion of the pump is picked off with a window upstream of the sample. This pick-off is then directed onto a camera pixel with no probe intensity. The intensity of this pick-off is used as a live readout for whether a spectrum is pumped or unpumped. Difference spectra ($\frac{T_{Pumped} - T_{Unpumped}}{T_{Unpumped}} = \frac{\Delta T}{T}$) are computed as a function of real exposure time, with the pump blocked for the first several seconds of the experiment to ensure there is no pump exposure prior to the start of the experiment. This experiment was repeated under varying pump conditions to investigate the effect of pump parameters (see the Supporting Information).

Transient Absorption. Transient absorption experiments on irradiated samples were conducted similarly to the real-time laser exposure experiments described above with the difference that the pump−probe time delay was varied from −30 to 500 ps, and that the pump was set at 640 nm and 50 $\mu J/cm^2$. The high pump fluence was chosen in order to rapidly induce the observed spectral modification, as well as collect high signal-to-noise difference spectra in a short window of exposure time.

https://doi.org/10.1021/acs.jpcc.4c04253
J. Phys. Chem. C 2024, 128, 17536−17542

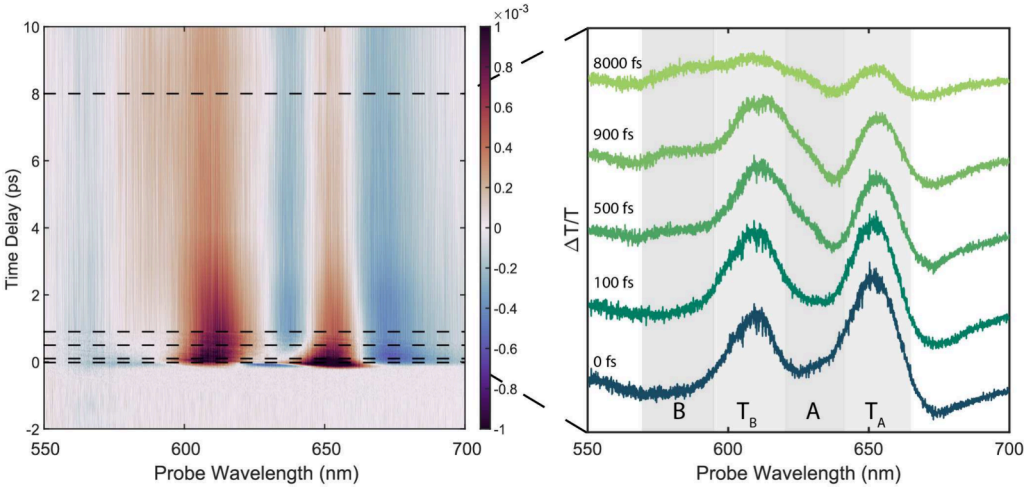

Figure 2. Transient absorption spectrum of monolayer MoS_2. The pump pulse was centered at 640 nm and set at a fluence of 50 $\mu J/cm^2$ in order to rapidly induce the spectral modification observed in the real-time experiment. Data were averaged for 25 cycles of acquisition (4 h). Pump−probe time delay was stepped alternately in positive and negative directions, such that time delay and real time are not monotonically correlated. Left: Contour plot of transient absorption experiment. Color bar is in $\Delta T/T$. Black dashed lines indicate pump−probe time delays shown on right. Right: line cuts of difference spectra at increasing pump−probe time delays. Shaded regions indicate two pairs of features labeled A and B, T_A and T_B. Spectra are vertically offset for clarity.

The particular behavior being analyzed here is qualitatively in agreement with that of lower pump fluences (see the Supporting Information), albeit more severe. A typical fitted signal rise time in transient absorption experiments is 50−70 fs.

Raman Mapping. A Raman spectral map was collected by rastering the sample. Spectra were collected using a Horiba LabRAM HR Evolution spectrometer equipped with a Horiba Synapse OE-CCD camera. The laser was centered at 532 nm and passed through a 25% neutral density filter. Each spectrum was collected over a 10 s acquisition time. A total of 441 spectra were acquired over a 500 μm by 500 μm area in steps of 25 μm. A 600 grooves/mm grating was used to achieve a spectral resolution of just under 2 cm^{-1}. Raster-scanned maps were obtained by translating the sample by motorized linear stages (Marzhauser) in the X and Y directions. All Raman spectra were collected at room temperature in ambient atmospheric conditions.

Sample Preparation. The MoS_2 sample was grown by metal−organic chemical vapor deposition (MOCVD) as described in detail by Kang et al.[29] MOCVD is a popular technique for growth of TMD monolayers, as it can produce large, wafer scale films.[30] Briefly, Molybdenum hexacarbonyl and diethyl sulfide act as the precursors for Mo and S, respectively. H_2 and Ar are injected into the chamber as carriers. The total chamber pressure was 7.5 Torr, at a temperature of 550 °C, and a growth time of 26 h. Samples are initially grown on Si/SiO_2. Following growth, samples are wet transferred onto transparent fused silica by delaminating the MoS_2 layer from the Si/SiO_2 substrate with water, then picking up the floating layer with fused silica.

RESULTS

Laser Exposure Experiments. In order to measure the effect of laser exposure, we collect transient difference spectra at a fixed pump−probe time delay as a function of real-time. Difference spectra are collected every 160 μs, and averaged in blocks of 50−100 s. An experimental schematic is shown in Figure 1a. We observe a real-time laser-induced modification of the transient difference spectrum of MoS_2 (Figure 1b). Monolayer MoS_2 mounted on fused silica was placed in an optical cryostat held at 78 K with the sample space under vacuum. The sample was irradiated with a narrowband (∼100 meV) pump pulse centered at 575 nm, and a broadband white light (800−500 nm) probe pulse. The difference spectrum, $\frac{\Delta T}{T}$, at a fixed pump−probe time delay of 2 ps was collected as a function of real-time laser exposure (see the Methods section for more details). Immediately upon pump exposure, ground state bleach signatures (positive signal) appear at 640 and 595 nm from the MoS_2 A and B excitons, respectively. Note, these positions are blue-shifted from their room temperature positions of 670 and 620 nm.[13,31,32] As real-time exposure increases, the A exciton blue-shifts on a time scale of several hundred seconds, followed by the appearance of a feature to the red, labeled T_A in Figure 1b, which becomes well resolved from the original excitonic feature after a few thousand seconds of laser exposure. At the same time, the B exciton becomes less spectrally distinct after a few hundred seconds of exposure, and is difficult to distinguish from noise after a few thousand seconds of exposure. This laser-induced modification is permanent. Following initial laser exposure, pump and probe were blocked for 1 h, after which the sample was re-exposed to light (Figure 1b, shaded region). Immediately upon re-exposure, the spectrum matches well with that of the end of the initial exposure experiment, rather than recovering.

Despite the appearance of these modifications in pump−probe data, this modification is not immediately apparent in the static absorption spectrum. Figure 1c shows the static absorption spectrum of a sample spot before (blue) and after (red) laser exposure. While peak intensities drop and shift slightly, there is no obvious evidence of additional peaks. Static absorption spectra are therefore insufficient to diagnose this type of laser-induced damage, making this effect more difficult to identify.

Transient Absorption. In order to assess the impact this laser-induced modification would have on an ultrafast time-resolved experiment, we performed transient absorption at a

https://doi.org/10.1021/acs.jpcc.4c04253
J. Phys. Chem. C 2024, 128, 17536−17542

high pump fluence. A time-resolved transient absorption experiment on laser-modified samples is shown in Figure 2, which reveals dynamics between the peaks that occur in laser-modified samples. A high fluence ($50\ \frac{\mu J}{cm^2}$) was used in the transient absorption experiment in order to rapidly induce the spectral modification observed in Figure 1, such that the difference spectra have already been severely modified by the onset of signal in this experiment. Figure 2 shows transient absorption difference spectra at a series of pump−probe time delays. At early times (bottom two spectra), only two features are clearly observed, labeled T_A (spectrally aligned with T_A in Figure 1b) and T_B. At 500 fs delay, additional features appear at 630 nm, labeled A, and at 580 nm, labeled B, which are slightly blue-shifted from initial A and B positions in Figure 1b. At late pump−probe time delays (several picoseconds and beyond), peaks A and B are of comparable intensity to peaks T_A and T_B. We note that the feature labeled T_A is the laser-induced feature, which appears only after several hundred seconds of laser exposure in Figure 1. In Figure 2, T_A and T_B are bleached at $\Delta t = 0$ fs, while A and B are bleached on a time delay. We hypothesize that after sufficient laser exposure (as is often required in a time-resolved experiment), the laser-induced T_A and T_B become the dominant features in transient absorption spectra, appearing at time zero, while the main excitonic features appear on a pump−probe time delay of a few picoseconds. Such a delayed appearance of a new feature is easy to misassign. For example, in van der Waals heterostructures, a feature appearing delayed from time zero could be indicative of a charge transfer process. Characterization of these features is therefore critical in order to distinguish laser-induced behavior from behavior intrinsic to a material.

Raman Mapping. We further characterize the effect of laser exposure on our sample using Raman spectral mapping (Figure 3). Raman spectra were collected over a 500 μm by 500 μm area in steps of 25 μm by raster scanning (see the Methods section for more details). Characteristic spectra of two regions, indicated with red and blue boxes, are shown in Figure 3a. There is an apparent shift in the A_{1g} mode between the two regions, indicated by the green dashed line in the inset of Figure 3a, and the appearance of a broad spectral feature in the at high wavenumbers in regions indicated by the red box. Iberi et al.[33] observed increased photoluminescence in a corresponding energy region on electron irradiated $MoSe_2$ and attributed this increase to the induction of defects.

DISCUSSION

We hypothesize that the laser-induced feature observed in these experiments corresponds to increased negative trion formation supported by laser-induced sulfur vacancy defects. Laser-induced chalcogen vacancies in TMD monolayers have been reported previously.[34] These vacancies are also common in as-grown MoS_2[35,36] and can be formed relatively easily via heating,[37] or irradiation with ions[38] or electrons.[39,40] Chalcogen vacancies are permanent, consistent with our results. Permanent vacancy formation should be more obvious in vacuum than in ambient conditions, as atmospheric oxygen and water can passivate chalcogen vacancies,[34,40−42] diminishing any vacancy-induced signatures. TMD chalcogen vacancies are also known to support the formation of negatively charged trions.[34] The spacing between induced and neutral exciton peaks of 50 meV is in agreement with the literature values for the spacing between the negative trion and neutral exciton.[19,43]

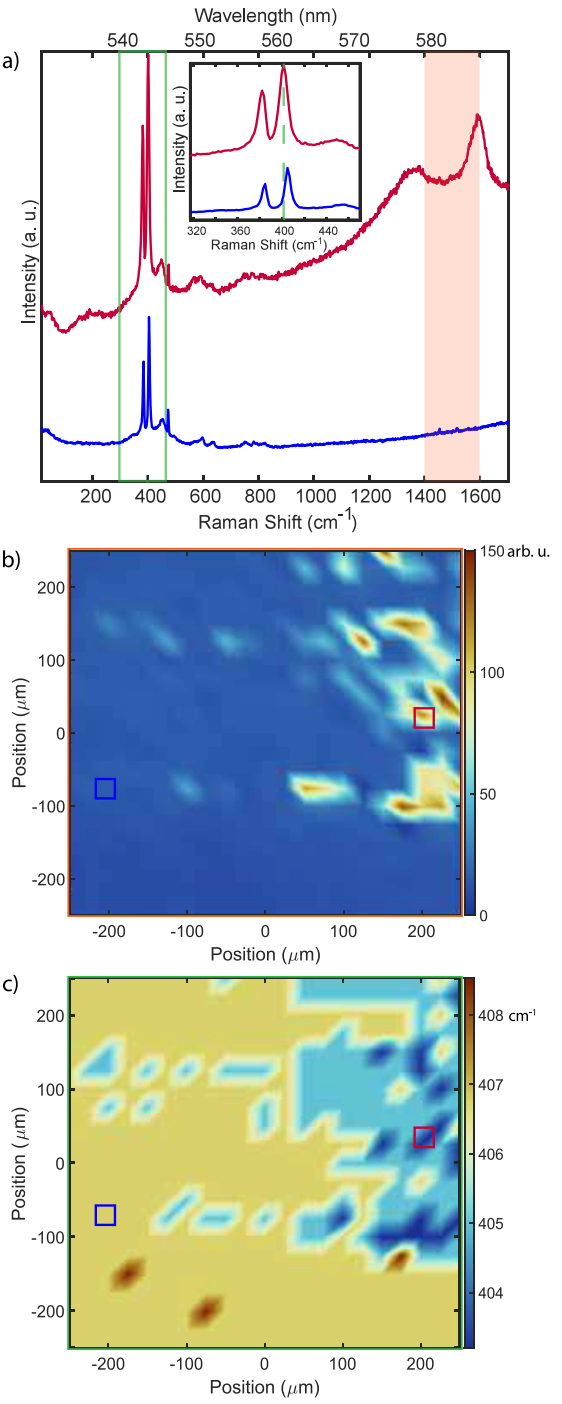

Figure 3. Raman spectra of MoS_2 samples after laser exposure experiments. (a) Representative Raman spectra at two positions (corresponding to matching colored boxes in (b) and (c)). Inset corresponds to green boxed region and shows the characteristic E_{2g} and A_{1g} modes. (b) Integrated intensity from 1400 to 1600 cm^{-1} (575 to 590 nm), corresponding to the orange shaded region in (a). (c) Position of the A_{1g} mode over real space.

A possible alternative assignment for the induced time-resolved feature is a defect localized exciton. A high density of defects, such as sulfur vacancies, would support the increased density of defect localized excitons. Defect localized excitons are also observed at low temperatures at lower energies than the corresponding free exciton.[32,44−46] However, these localized excitons have a reported spacing of 90 meV from the main

https://doi.org/10.1021/acs.jpcc.4c04253
J. Phys. Chem. C 2024, 128, 17536−17542

excitonic feature,[44−46] which is larger than the spacing of 50 meV observed in our experiments. The small energy difference between the trion and exciton also explains why this phenomenon is more challenging to resolve in the static absorption spectra.

The hypothesis of trion formation is also consistent with the observed blue-shifting of the neutral exciton resonances during laser exposure. Disruption of the crystal structure due to the induction of vacancies (and potentially other defects) could reduce the exciton binding energy, resulting in a blue-shifted peak.

Our assignment of laser-induced sulfur vacancies is further supported by the Raman mapping results. The A_{1g} mode of MoS_2 is known to red-shift in regions of high defect density,[39,47] and the photoluminescence in the corresponding energy region has been reported to increase in regions of high chalcogen vacancy density in $MoSe_2$,[33] in agreement Figure 3a. Figures 3b and 3c show 2D maps as a function of real space of the integrated intensity from 1400 to 1600 cm^{-1}, and position of the A_{1g} mode, respectively. The two maps appear spatially correlated, suggesting that the same structural effect is responsible for the spatial variation. Sequential laser exposure experiments were conducted by translating the sample and cryostat assembly on a linear stage in steps of 200 μm. The beam spot size in each experiment was on the order of 100 μm in diameter. This is consistent with the apparent line of affected spots running vertically along the right-hand side of Figures 3b and c. Similar maps were taken of a sample that had not been exposed to pulsed laser irradiation, and showed a more uniform and less correlated result (see the Supporting Information). This supports our assignment of the spectral modification as laser-induced sulfur vacancies.

We therefore propose that the induced feature is a negative trion, possibly localized to defects.[48] A cartoon depicting the process by which the spectra are modified is shown in Figure 4. Sulfur vacancies serve to n-dope the MoS_2, drawing excess electrons from the underlying substrate,[41,49,50] supporting the formation of negative trions[49] upon photoexcitation. Dissociation of trions into neutral excitons and free electrons has been reported,[49,51] which could correspond to the observed slow rise of the main excitonic feature in transient absorption. We believe that there is a defect density threshold at which the initially pumped species switch from being neutral exicton dominated to trion dominated (see the Supporting Information) and that this effect will be influenced by both the substrate and the intrinsic defect density of the sample.

Previous investigations on the impact of laser-induced chalcogen vacancies on the dynamics of MoS_2 have used much higher fluences than reported here.[52] Our results here represent a distinct regime, in which spectra are modified slowly under fluences that are representative of actual experimental conditions, and must therefore be considered when performing such experiments. Generally researchers either (1) assume that samples are unaffected by experiments or (2) quantify the alterations or damage with static absorption spectra. It is evident that not only is a laser-induced change possible under realistic conditions, but also that static spectra are insufficient to determine whether that change is significant to the measurement. The rate of spectral modification we observe here is dependent on pump conditions (color, fluence, repetition rate, etc.), but the qualitative nature of the modification itself is consistent (see the Supporting Information). Similarly, we expect the strength and rate of this

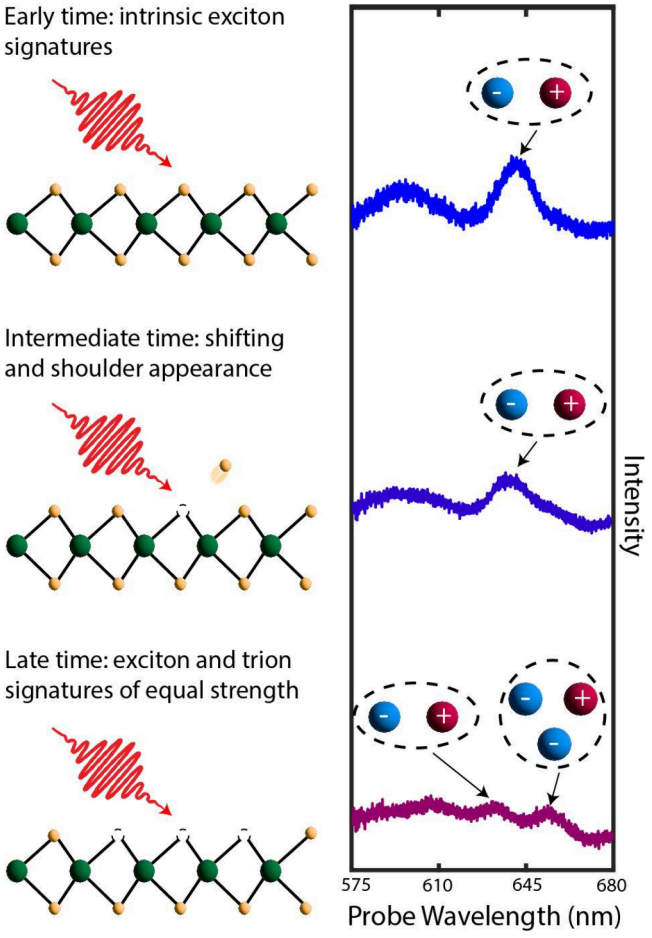

Figure 4. Cartoon depicting the formation of sulfur vacancies during laser irradiation and the resulting spectral modification. Spectra shown are those obtained from real-time laser exposure experiments (see Figure 1b).

modification to be dependent on both the nature of the sample (e.g., grain size, intrinsic defect density, oxidation, encapsulation) and sample environment (e.g., vacuum versus exchange gas versus atmosphere). Due to the nature of CVD and MOCVD, as well as the volatility of chalcogens, control over the defect density of as-grown monolayer TMDs is infeasible. The observed spectral modification may or may not therefore be present to a detectable degree in all optical experiments, as is clear from the current body of literature. We do, however, believe that it is possible to observe this spectral modification in any optical experiment on thin film TMDs, and it is therefore important to consider such laser-induced modification when interpreting data.

CONCLUSION

Through a series of optical experiments, we have characterized and assigned the signatures of laser-induced modification of monolayer MoS_2 which can appear during transient absorption and other pulsed laser experiments. A pulsed pump laser leads to the formation of sulfur vacancy defects, resulting in the appearance of features that are not present intrinsically. This assignment is supported by the permanence of the effect, indicative of a physical modification, and by Raman mapping results. These defects serve to n-dope the sample. The highly doped system supports the formation of negative trions, which

https://doi.org/10.1021/acs.jpcc.4c04253
J. Phys. Chem. C 2024, 128, 17536−17542

manifest in transient absorption experiments as the appearance of an additional ground state bleach feature. After sufficient laser-induced damage, the trions become the dominant time-resolved feature in transient spectra, while neutral excitons form by the dissociation of trions into excitons and free electrons. This results in the appearance of the ground state bleach of neutral excitons occurring on a time delay with respect to the bleach of negative trions, a behavior which could potentially be mistaken for charge transfer in a van der Waals heterostructure.

We report this behavior here in order to aid in the accuracy of assignments in future optical experiments on thin film TMDs and related systems. Transient absorption data requires significant interpretation and analysis in order to draw physically meaningful conclusions. Having a more complete understanding of possible assignments will help to facilitate this analysis. We recognize that many factors may affect the degree to which this behavior may influence measurements; further research should focus on quantifying the effect of intrinsic defect densities and experimental environment conditions on this phenomenon.

■ ASSOCIATED CONTENT

Supporting Information

The Supporting Information is available free of charge at https://pubs.acs.org/doi/10.1021/acs.jpcc.4c04253.

Variations on experimental conditions described in main text, Raman map comparison to control sample, description of the temporal chirp correction process employed in main text (PDF)

■ AUTHOR INFORMATION

Corresponding Author

Sarah B. King − *Department of Chemistry and James Franck Institute, University of Chicago, Chicago, Illinois 60637, United States;* orcid.org/0000-0003-0274-9894; Email: sbking@uchicago.edu

Authors

Clare L. Keenan − *Department of Chemistry and James Franck Institute, University of Chicago, Chicago, Illinois 60637, United States;* orcid.org/0000-0001-5652-2068

Ashley Arcidiacono − *James Franck Institute, University of Chicago, Chicago, Illinois 60637, United States;* orcid.org/0000-0001-8617-2097

Nasim Mirzajani − *Department of Chemistry and James Franck Institute, University of Chicago, Chicago, Illinois 60637, United States*

Cooper R. Johnston − *Department of Chemistry and James Franck Institute, University of Chicago, Chicago, Illinois 60637, United States*

Complete contact information is available at: https://pubs.acs.org/10.1021/acs.jpcc.4c04253

Notes

The authors declare no competing financial interest.

■ ACKNOWLEDGMENTS

The authors thank Prof. Jiwoong Park, Ce Liang, Dr. Tomojit Chowdhury, and Zehra Naqvi for preparing samples, Dr. Justin Jureller and Dr. Sarah Brown for maintenance of, and assistance with, the Raman spectrometer used in these experiments, and Prof. Greg Engel for loan of cryostat equipment for early stage experiments. This work was funded the Arnold and Mabel Beckman Foundation (Beckman Young Investigators Program) and by the Research Corporation for Scientific Advancement (Cottrell Scholars Program). A.A. acknowledges support by the Arnold and Mabel Beckman Foundation (A. O. Beckman Postdoctoral Fellowship). This work made use of the shared facilities at the University of Chicago Materials Research Science and Engineering Center, supported by the National Science Foundation under Award DMR-2011854.

■ REFERENCES

(1) Liu, Y.; Lin, L.; Sun, H.-B. Optical Modification of Two-Dimensional Materials: From Atomic to Electronic Scale. *J. Phys. Chem. C* **2024**, *128*, 2271−2290.

(2) Zheng, W.; Jiang, Y.; Hu, X.; Li, H.; Zeng, Z.; Wang, X.; Pan, A. Light Emission Properties of 2D Transition Metal Dichalcogenides: Fundamentals and Applications. *Adv. Opt. Mater.* **2018**, *6*, 1800420.

(3) Huang, Y. L.; Zheng, Y. J.; Song, Z.; Chi, D.; Wee, A. T. S.; Quek, S. Y. The organic−2D transition metal dichalcogenide heterointerface. *Chem. Soc. Rev.* **2018**, *47*, 3241−3264.

(4) Novoselov, K. S.; Mishchenko, A.; Carvalho, A.; Neto, A. H. C. 2D materials and van der Waals heterostructures. *Science* **2016**, *353*, No. aac9439.

(5) Gupta, A.; Sakthivel, T.; Seal, S. Recent development in 2D materials beyond graphene. *Prog. Mater. Sci.* **2015**, *73*, 44−126.

(6) Tan, C.; Cao, X.; Wu, X.-J.; He, Q.; Yang, J.; Zhang, X.; Chen, J.; Zhao, W.; Han, S.; Nam, G.-H.; et al. Recent Advances in Ultrathin Two-Dimensional Nanomaterials. *Chem. Rev.* **2017**, *117*, 6225−6331.

(7) Bhimanapati, G. R.; Lin, Z.; Meunier, V.; Jung, Y.; Cha, J.; Das, S.; Xiao, D.; Son, Y.; Strano, M. S.; Cooper, V. R.; et al. Recent Advances in Two-Dimensional Materials beyond Graphene. *ACS Nano* **2015**, *9*, 11509−11539.

(8) Deng, S.; Snaider, J. M.; Gao, Y.; Shi, E.; Jin, L.; Schaller, R. D.; Dou, L.; Huang, L. Long-lived charge separation in two-dimensional ligand-perovskite heterostructures. *J. Chem. Phys.* **2020**, *152*, No. 044711.

(9) Zhou, F.; Hwangbo, K.; Zhang, Q.; Wang, C.; Shen, L.; Zhang, J.; Jiang, Q.; Zong, A.; Su, Y.; Zajac, M.; et al. Dynamical criticality of spin-shear coupling in van der Waals antiferromagnets. *Nat. Commun.* **2022**, *13*, 6598.

(10) Mak, K. F.; Lee, C.; Hone, J.; Shan, J.; Heinz, T. F. Atomically Thin MoS2: A New Direct-Gap Semiconductor. *Phys. Rev. Lett.* **2010**, *105*, 136805.

(11) Kafle, T. R.; Kattel, B.; Lane, S. D.; Wang, T.; Zhao, H.; Chan, W.-L. Charge Transfer Exciton and Spin Flipping at Organic−Transition-Metal Dichalcogenide Interfaces. *ACS Nano* **2017**, *11*, 10184−10192.

(12) Wang, Q. H.; Kalantar-Zadeh, K.; Kis, A.; Coleman, J. N.; Strano, M. S. Electronics and optoelectronics of two-dimensional transition metal dichalcogenides. *Nat. Nanotechnol.* **2012**, *7*, 699−712.

(13) Chi, Z.; Chen, H.; Chen, Z.; Zhao, Q.; Chen, H.; Weng, Y.-X. Ultrafast Energy Dissipation via Coupling with Internal and External Phonons in Two-Dimensional MoS2. *ACS Nano* **2018**, *12*, 8961−8969.

(14) Wang, W.; Sui, N.; Chi, X.; Kang, Z.; Zhou, Q.; Li, L.; Zhang, H.; Gao, J.; Wang, Y. Investigation of Hot Carrier Cooling Dynamics in Monolayer MoS2. *J. Phys. Chem. Lett.* **2021**, *12*, 861−868.

(15) Yuan, L.; Wang, T.; Zhu, T.; Zhou, M.; Huang, L. Exciton Dynamics, Transport, and Annihilation in Atomically Thin Two-Dimensional Semiconductors. *J. Phys. Chem. Lett.* **2017**, *8*, 3371−3379.

(16) Nie, Z.; Long, R.; Teguh, J. S.; Huang, C.-C.; Hewak, D. W.; Yeow, E. K. L.; Shen, Z.; Prezhdo, O. V.; Loh, Z.-H. Ultrafast Electron and Hole Relaxation Pathways in Few-Layer MoS2. *J. Phys. Chem. C* **2015**, *119*, 20698−20708.

(17) Wibmer, L.; Lages, S.; Unruh, T.; Guldi, D. M. Excitons and Trions in One-Photon- and Two-Photon-Excited MoS2: A Study in Dispersions. *Adv. Mater.* **2018**, *30*, No. e1706702.
(18) Trovatello, C.; Katsch, F.; Li, Q.; Zhu, X.; Knorr, A.; Cerullo, G.; Dal Conte, S. Disentangling Many-Body Effects in the Coherent Optical Response of 2D Semiconductors. *Nano Lett.* **2022**, *22*, 5322−5329.
(19) Genco, A.; Trovatello, C.; Louca, C.; Watanabe, K.; Taniguchi, T.; Tartakovskii, A. I.; Cerullo, G.; Dal Conte, S. Ultrafast Exciton and Trion Dynamics in High-Quality Encapsulated MoS2Monolayers. *Phys. Status Solidi B* **2023**, *260*, 2200376.
(20) Cunningham, P. D.; Hanbicki, A. T.; McCreary, K. M.; Jonker, B. T. Photoinduced Bandgap Renormalization and Exciton Binding Energy Reduction in WS2. *ACS Nano* **2017**, *11*, 12601−12608.
(21) Barbone, M.; Montblanch, A. R.-P.; Kara, D. M.; Palacios-Berraquero, C.; Cadore, A. R.; Fazio, D. D.; Pingault, B.; Mostaani, E.; Li, H.; Chen, B.; et al. Charge-tuneable biexciton complexes in monolayer WSe2. *Nat. Commun.* **2018**, *9*, 3721.
(22) de Clercq, D. M.; Yang, J.; Hanif, M.; Alves, J.; Feng, J.; Nielsen, M. P.; Kalantar-Zadeh, K.; Schmidt, T. W. Exciton Dissociation, Charge Transfer, and Exciton Trapping at the MoS2/Organic Semiconductor Interface. *J. Phys. Chem. C* **2023**, *127*, 11260−11267.
(23) Gu, J.; Walther, V.; Waldecker, L.; Rhodes, D.; Raja, A.; Hone, J. C.; Heinz, T. F.; Kéna-Cohen, S.; Pohl, T.; Menon, V. M. Enhanced nonlinear interaction of polaritons via excitonic Rydberg states in monolayer WSe2. *Nat. Commun.* **2021**, *12*, 2269.
(24) Zhou, J.; Thomas, J. C.; Barre, E.; Barnard, E. S.; Raja, A.; Cabrini, S.; Munechika, K.; Schwartzberg, A.; Weber-Bargioni, A. Near-Field Coupling with a Nanoimprinted Probe for Dark Exciton Nanoimaging in Monolayer WSe2. *Nano Lett.* **2023**, *23*, 4901−4907.
(25) Raoufi, M.; Chandrabose, S.; Wang, R.; Sun, B.; Morales, N. Z.; Shoaee, S.; Blumstengel, S.; Koch, N.; List-Kratochvil, E.; Neher, D. Influence of the Energy Level Alignment on Charge Transfer and Recombination at the Monolayer-MoS2/Organic Hybrid Interface. *J. Phys. Chem. C* **2023**, *127*, 5866−5875.
(26) Sim, S.; Park, J.; Song, J.-G.; In, C.; Lee, Y.-S.; Kim, H.; Choi, H. Exciton dynamics in atomically thin MoS2: Interexcitonic interaction and broadening kinetics. *Phys. Rev. B* **2013**, *88*, No. 075434.
(27) Aleithan, S. H.; Livshits, M. Y.; Khadka, S.; Rack, J. J.; Kordesch, M. E.; Stinaff, E. Broadband femtosecond transient absorption spectroscopy for a CVD MoS2 monolayer. *Phys. Rev. B* **2016**, *94*, No. 035445.
(28) Homan, S. B.; Sangwan, V. K.; Balla, I.; Bergeron, H.; Weiss, E. A.; Hersam, M. C. Ultrafast Exciton Dissociation and Long-Lived Charge Separation in a Photovoltaic Pentacene−MoS2 van der Waals Heterojunction. *Nano Lett.* **2017**, *17*, 164−169.
(29) Kang, K.; Xie, S.; Huang, L.; Han, Y.; Huang, P. Y.; Mak, K. F.; Kim, C.-J.; Muller, D.; Park, J. High-mobility three-atom-thick semiconducting films with wafer-scale homogeneity. *Nature* **2015**, *520*, 656−660.
(30) Hossen, M. F.; Shendokar, S.; Aravamudhan, S. Defects and Defect Engineering of Two-Dimensional Transition Metal Dichalcogenide (2D TMDC) Materials. *Nanomaterials* **2024**, *14*, 410.
(31) Verhagen, T.; Guerra, V. L. P.; Haider, G.; Kalbac, M.; Vejpravova, J. Towards the evaluation of defects in MoS 2 using cryogenic photoluminescence spectroscopy. *Nanoscale* **2020**, *12*, 3019−3028.
(32) Pandey, J.; Soni, A. Unraveling biexciton and excitonic excited states from defect bound states in monolayer MoS2. *Appl. Surf. Sci.* **2019**, *463*, 52−57.
(33) Iberi, V.; Liang, L.; Ievlev, A. V.; Stanford, M. G.; Lin, M.-W.; Li, X.; Mahjouri-Samani, M.; Jesse, S.; Sumpter, B. G.; Kalinin, S. V.; et al. Nanoforging Single Layer MoSe2 Through Defect Engineering with Focused Helium Ion Beams. *Sci. Rep.* **2016**, *6*, 30481.
(34) Huang, G.-Y.; Lin, L.; Zhao, S.; Li, W.; Deng, X.; Zhang, S.; Wang, C.; Li, X.-Z.; Zhang, Y.; Fang, H.-H.; et al. All-Optical Reconfigurable Excitonic Charge States in Monolayer MoS2. *Nano Lett.* **2023**, *23*, 1514−1521.
(35) Gao, L.; Hu, Z.; Lu, J.; Liu, H.; Ni, Z. Defect-related dynamics of photoexcited carriers in 2D transition metal dichalcogenides. *Phys. Chem. Chem. Phys.* **2021**, *23*, 8222−8235.
(36) Aliyar, T.; Ma, H.; Krishnan, R.; Singh, G.; Chong, B. Q.; Wang, Y.; Verzhbitskiy, I.; Wong, C. P. Y.; Goh, K. E. J.; Shen, Z. X.; et al. Symmetry Breaking and Spin−Orbit Coupling for Individual Vacancy-Induced In-Gap States in MoS2Monolayers. *Nano Lett.* **2024**, *24*, 2142−2148.
(37) Mitterreiter, E.; Schuler, B.; Micevic, A.; Hernangómez-Pérez, D.; Barthelmi, K.; Cochrane, K. A.; Kiemle, J.; Sigger, F.; Klein, J.; Wong, E.; et al. The role of chalcogen vacancies for atomic defect emission in MoS2. *Nat. Commun.* **2021**, *12*, 3822.
(38) Hötger, A.; Amit, T.; Klein, J.; Barthelmi, K.; Pelini, T.; Delhomme, A.; Rey, S.; Potemski, M.; Faugeras, C.; Cohen, G.; et al. Spin-defect characteristics of single sulfur vacancies in monolayer MoS2. *npj 2D Mater Appl* **2023**, *7*, 30.
(39) Parkin, W. M.; Balan, A.; Liang, L.; Das, P. M.; Lamparski, M.; Naylor, C. H.; Rodriguez-Manzo, J. A.; Johnson, A. T. C.; Meunier, V.; Drndic, M. Raman Shifts in Electron-Irradiated Monolayer MoS2. *ACS Nano* **2016**, *10*, 4134−4142.
(40) Komsa, H.-P.; Kotakoski, J.; Kurasch, S.; Lehtinen, O.; Kaiser, U.; Krasheninnikov, A. V. Two-Dimensional Transition Metal Dichalcogenides under Electron Irradiation: Defect Production and Doping. *Phys. Rev. Lett.* **2012**, *109*, No. 035503.
(41) Bera, A.; Muthu, D. V. S.; Sood, A. K. Enhanced Raman and photoluminescence response in monolayer MoS2 due to laser healing of defects. *J. Raman Spectrosc.* **2018**, *49*, 100−105.
(42) Lu, J.; Carvalho, A.; Chan, X. K.; Liu, H.; Liu, B.; Tok, E. S.; Loh, K. P.; Neto, A. H. C.; Sow, C. H. Atomic Healing of Defects in Transition Metal Dichalcogenides. *Nano Lett.* **2015**, *15*, 3524−3532.
(43) Mak, K. F.; He, K.; Lee, C.; Lee, G. H.; Hone, J.; Heinz, T. F.; Shan, J. Tightly bound trions in monolayer MoS2. *Nat. Mater.* **2013**, *12*, 207−211.
(44) Korn, T.; Heydrich, S.; Hirmer, M.; Schmutzler, J.; Schüller, C. Low-temperature photocarrier dynamics in monolayer MoS2. *Appl. Phys. Lett.* **2011**, *99*, 102109.
(45) Saigal, N.; Ghosh, S. Evidence for two distinct defect related luminescence features in monolayer MoS2. *Appl. Phys. Lett.* **2016**, *109*, 122105.
(46) Li, H.; Zhang, X. Temperature-dependent photoluminescence and time-resolved photoluminescence study of monolayer molybdenum disulfide. *Opt. Mater.* **2020**, *107*, 110150.
(47) Kao, M.-Y.; Hsu, C.-H.; Huang, Y.-Q.; Hsu, Y.-C.; Liu, M.-J.; Chen, C.-T.; Lai, P.-C.; Lu, M.-Y.; Wu, P.-J.; Chueh, Y.-L. Effects of Extreme Ultraviolet Radiation on Transition Metal Dichalcogenides: Investigation of Physical and Electrical Properties. *ACS Appl. Electron. Mater.* **2024**, Article ASAP.
(48) Sebait, R.; Biswas, C.; Song, B.; Seo, C.; Lee, Y. H. Identifying Defect-Induced Trion in Monolayer WS2 via Carrier Screening Engineering. *ACS Nano* **2021**, *15*, 2849−2857.
(49) Golovynskyi, S.; Datsenko, O. I.; Dong, D.; Lin, Y.; Irfan, I.; Li, B.; Lin, D.; Qu, J. Trion Binding Energy Variation on Photoluminescence Excitation Energy and Power during Direct to Indirect Bandgap Crossover in Monolayer and Few-Layer MoS2. *J. Phys. Chem. C* **2021**, *125*, 17806−17819.
(50) Bao, W.; Borys, N. J.; Ko, C.; Suh, J.; Fan, W.; Thron, A.; Zhang, Y.; Buyanin, A.; Zhang, J.; Cabrini, S.; et al. Visualizing nanoscale excitonic relaxation properties of disordered edges and grain boundaries in monolayer molybdenum disulfide. *Nat. Commun.* **2015**, *6*, 7993.
(51) Ayari, S.; Jaziri, S.; Ferreira, R.; Bastard, G. Phonon-assisted exciton/trion conversion efficiency in transition metal dichalcogenides. *Phys. Rev. B* **2020**, *102*, 125410.
(52) Pan, C.; Jiang, L.; Sun, J.; Wang, Q.; Wang, F.; Wang, K.; Lu, Y.; Wang, Y.; Qu, L.; Cui, T. Ultrafast optical response and ablation mechanisms of molybdenum disulfide under intense femtosecond laser irradiation. *Light Sci. Appl.* **2020**, *9*, 80.

https://doi.org/10.1021/acs.jpcc.4c04253
J. Phys. Chem. C 2024, 128, 17536−17542